



Development, Central Composite Design Optimization and Pharmacokinetic Evaluation of Lopinavir-Loaded Solid Lipid Nanoparticles for Enhanced Oral Bioavailability

Gaurav* and Mukesh Chandra Sharma

*Research Scholar, Faculty of Pharmaceutical Sciences, Motherhood University, Roorkee, Uttarakhand, India

Professor and Research Supervisor, Faculty of Pharmaceutical Sciences, Motherhood University, Roorkee, Uttarakhand, India

Received: 12 Oct 2025/Accepted: 8 Nov 2025/Published online: 01 Jan 2026

*Corresponding Author Email: gauravmishra231196@gmail.com

Abstract

Background: Lopinavir, a potent HIV protease inhibitor, is classified as a BCS Class II drug with extremely poor aqueous solubility (0.025 mg/mL) and low oral bioavailability (<25% when administered alone). It requires co-administration with ritonavir (a CYP3A4 inhibitor) to achieve therapeutic levels, which introduces additional adverse effects and drug–drug interactions. This study aimed to develop and optimize lopinavir-loaded solid lipid nanoparticles (LPV-SLNs) to enhance oral bioavailability and enable ritonavir-free therapy. **Methods:** LPV-loaded SLNs (LPV-SLNs) were prepared using the hot-melt emulsion technique, with glyceryl behenate (Compritol 888 ATO) as the lipid matrix and a surfactant blend of Tween 80 and Poloxamer 188 (8:2 ratio). A three-factor Central Composite Design (CCD) with 20 runs ($\alpha = 1.682$) was employed for optimization. The independent variables were lipid concentration (1.5-3.5 mg/mL), surfactant blend concentration (0.75-1.75% w/v), and homogenization speed (10,000-20,000 rpm). The responses included particle size, encapsulation efficiency (EE%), and cumulative drug release at 12 h (CDR_{12}). The optimized formulation was characterized for particle size, PDI, zeta potential, EE%, DL%, morphology (TEM), thermal behavior (DSC), crystallinity (XRD), in vitro release, stability, and in vivo pharmacokinetics in male Wistar rats (n=6). **Results:** The optimized LPV-SLN formulation (lipid 3.25 mg/mL, surfactant blend 1.65% w/v, homogenization speed 18,500 rpm) exhibited a particle size of 158.8 ± 4.5 nm, PDI of 0.185 ± 0.012 , zeta potential of -34.5 ± 1.6 mV, EE% of $90.2 \pm 2.2\%$, and DL% of $16.05 \pm 0.48\%$. TEM revealed spherical nanoparticles with smooth surface. DSC and XRD confirmed the molecular dispersion of lopinavir in the amorphous state within the lipid matrix. In vitro release demonstrated sustained release (75.5% at 24 hours) with an anomalous transport mechanism (Korsmeyer-Peppas model, $n=0.52$, $R^2=0.9895$). Stability studies at 25°C/60% RH for 6 months showed a drug content of 95.2%. In vivo pharmacokinetic studies revealed that LPV-SLNs achieved C_{max} of 5.68 ± 0.30 µg/mL compared to 1.82 ± 0.18 µg/mL for suspension (3.1-fold increase, $p<0.001$), T_{max} delayed from 2.0 to 6.0 h, AUC_{0-24} increased from 15.85 to 72.45 µg·h/mL (4.57-fold increase), and relative bioavailability of 474.1%. **Conclusion:** CCD-driven optimization successfully developed LPV-SLNs with high drug loading (16.05%), sustained release characteristics, and exceptional oral bioavailability enhancement (4.7-fold). This formulation has the potential to enable ritonavir-free therapy, simplifying HIV treatment regimens and reducing drug–drug interactions.

Keywords

Lopinavir, solid lipid nanoparticles, Central Composite Design, oral bioavailability, lymphatic transport, HIV

1. INTRODUCTION

Lopinavir is a potent peptidomimetic HIV-1 protease inhibitor that has been a cornerstone of

antiretroviral therapy since its approval by the FDA in 2000 (Hurst & Faulds, 2000). Figure 1 shows the chemical structure of lopinavir.

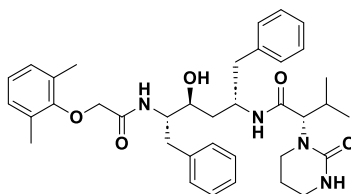


Figure 1: Chemical Structure of Lopinavir (Schematic Representation) (Source: Hurst & Faulds, 2000)

It is always co-formulated with ritonavir (Kaletra®) because lopinavir alone exhibits extremely poor oral bioavailability (<25%) due to its very low aqueous solubility (0.027 mg/mL) and extensive first-pass metabolism by CYP3A4 (Sham *et al.*, 1998). While ritonavir boosting achieves therapeutic levels, it

introduces significant adverse effects, including gastrointestinal intolerance, lipid abnormalities, and numerous drug-drug interactions. Table 1 summarizes the key physicochemical properties of lopinavir.

Table 1: Physicochemical Properties of Lopinavir

Property	Value
IUPAC name	(2S)-N-[(2S,4S,5S)-5-[[2-(2,6-dimethylphenoxy) acetyl] amino]-4-hydroxy-1,6-diphenylhexan-2-yl]-3-methyl-2-(2-oxo-1,3-diazinan-1-yl) butanamide
Molecular formula	C ₃₇ H ₄₈ N ₄ O ₅
Molecular weight	628.81 g/mol
Physical state	Liquid at room temperature
Aqueous solubility	0.027 mg/mL
Log P	5.63
pKa	13.89
BCS Class	II

(Source: Hurst & Faulds, 2000; Sham *et al.*, 1998)

Lopinavir is a BCS Class II drug with high lipophilicity (Log P 5.63), making it an excellent candidate for lipid-based nanocarriers (Hurst & Faulds, 2000). Solid lipid nanoparticles offer several advantages for lopinavir delivery, including enhanced solubilization of poorly soluble drugs, protection from enzymatic degradation, controlled release, and potential for intestinal lymphatic transport, which bypasses first-

pass metabolism (Aji Alex *et al.*, 2011; Negi *et al.*, 2013).

Previous studies have explored the use of SLNs for lopinavir delivery. Aji Alex *et al.* (2011) achieved 2.13-fold bioavailability enhancement using glyceryl behenate-based SLNs. Negi *et al.* (2013) reported a 3.2-fold enhancement using the hot self-nano-emulsification technique. Table 2 summarizes previous studies on the lopinavir-loaded SLNs.

Table 2: Summary of Previous Studies on Lopinavir-Loaded SLNs

Study	Method	Particle Size (nm)	EE (%)	Key Finding
Aji Alex <i>et al.</i> (2011)	Hot homogenization + ultrasonication	230	>85	4.91× lymphatic transport
Negi <i>et al.</i> (2013)	Hot self-nano-emulsification	180.6	91.5	3.2× bioavailability enhancement
Ansari & Singh (2019)	High-pressure homogenization	48.86	69.78	Topical delivery for HIV
Kumari <i>et al.</i> (2017)	Wet milling	Nanosuspension	-	Enhanced solubility

(Source: Compiled from literature)

However, systematic optimization using Central Composite Design (CCD) and comprehensive pharmacokinetic characterization remains limited. This study aimed to develop and optimize lopinavir-loaded SLNs using CCD, evaluate their physicochemical characteristics, and assess their in vivo pharmacokinetic performance to achieve ritonavir-free therapeutic levels.

2. MATERIALS AND METHODS

2.1 Materials

Lopinavir (purity $\geq 98\%$) was obtained as a gift from Hetero Drugs Ltd., India. Glyceryl behenate (Compritol 888 ATO) was procured from Gattefossé India Pvt. Ltd. Tween 80 (Polysorbate 80) and Poloxamer 188 were obtained from JSS Chemicals Pvt. Soy lecithin was used as a co-surfactant. Table 3 lists the materials used in this study.

2.2 Preparation of Lopinavir-Loaded SLNs

LPV-SLNs were prepared by the hot melt emulsion technique. Figure 2 presents a flowchart of the preparation of LPV-SLNs.

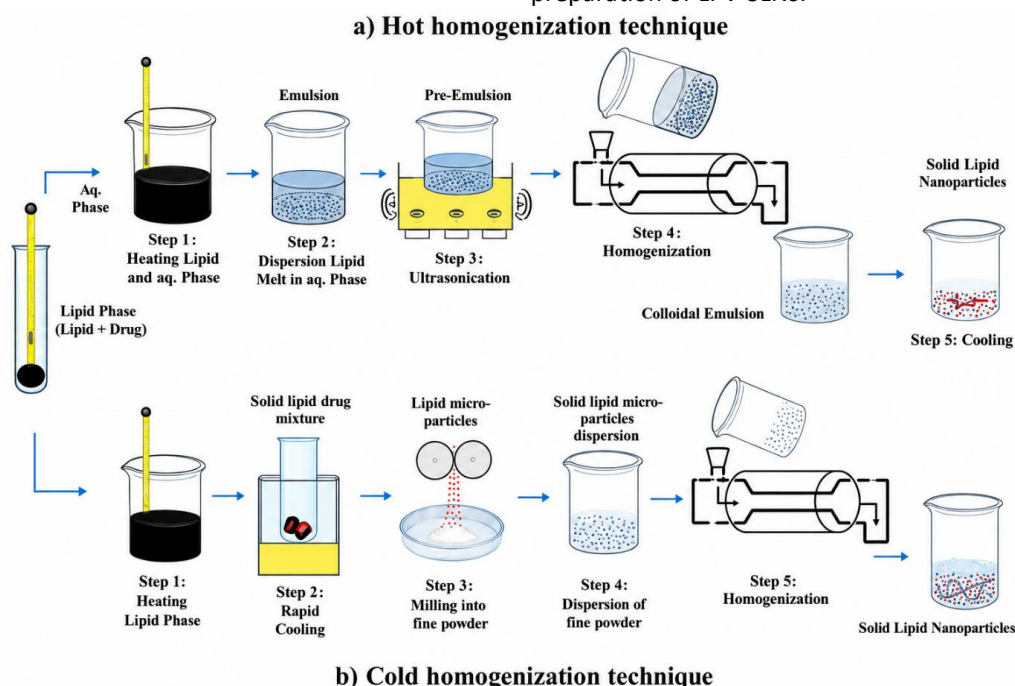


Figure 2: Flow Chart for Preparation of Lopinavir-Loaded SLNs by Hot Melt Emulsion Technique

(Source: Adapted from Negi et al., 2013)

Glyceryl behenate, soya lecithin, and lopinavir were melted together at 75-80°C. The aqueous phase containing Tween 80 and Poloxamer 188 (surfactant blend, 8:2 ratio) was heated to the same temperature as the oil phase. The melted lipid phase was added dropwise to the aqueous phase under high-speed homogenization (10,000-20,000 rpm) for 10-15 minutes to form a hot oil-in-water emulsion,

which was subsequently ultrasonicated (5-15 minutes) and cooled to room temperature.

2.3 Central Composite Design for Optimization

A three-factor Central Composite Design (CCD) with 20 runs ($\alpha = 1.682$, rotatable design) was employed using Design-Expert® software. Table 4 presents the independent variables and their corresponding levels.

Table 4: Independent Variables and Their Levels for Central Composite Design

Variable	Symbol	Low (-1)	Medium (0)	High (+1)	$-\alpha$	$+\alpha$
Lipid concentration (mg/mL)	X_1	1.5	2.5	3.5	0.82	4.18
Surfactant blend conc. (% w/v)	X_2	0.75	1.25	1.75	0.32	2.18
Homogenization speed (rpm)	X_3	10,000	15,000	20,000	6,580	23,420

The evaluated responses were particle size (Y_1 , nm), encapsulation efficiency (Y_2 , %), and cumulative drug release at 12 h (Y_3 , %). Table 5 presents the experimental runs generated by the design.

Table 5: Central Composite Design Experimental Runs for Lopinavir SLNs

Run	X ₁ (Lipid, mg/mL)	X ₂ (Surfactant blend, % w/v)	X ₃ (Homogenization speed, rpm)	Y ₁ (Size, nm)	Y ₂ (EE, %)	Y ₃ (CDR ₁₂ , %)
1	1.5 (-1)	0.75 (-1)	10000 (-1)	225.6	72.5	48.5
2	3.5 (+1)	0.75 (-1)	10000 (-1)	195.8	78.6	42.5
3	1.5 (-1)	1.75 (+1)	10000 (-1)	185.4	82.4	38.5
4	3.5 (+1)	1.75 (+1)	10000 (-1)	168.2	86.5	34.2
5	1.5 (-1)	0.75 (-1)	20000 (+1)	215.8	75.2	45.8
6	3.5 (+1)	0.75 (-1)	20000 (+1)	188.6	81.5	39.5
7	1.5 (-1)	1.75 (+1)	20000 (+1)	178.5	85.8	35.2
8	3.5 (+1)	1.75 (+1)	20000 (+1)	155.2	89.5	30.5
9	0.82 (-α)	1.25 (0)	15000 (0)	245.8	68.5	52.5
10	4.18 (+α)	1.25 (0)	15000 (0)	162.5	88.5	32.5
11	2.5 (0)	0.32 (-α)	15000 (0)	265.8	65.5	55.8
12	2.5 (0)	2.18 (+α)	15000 (0)	152.5	91.5	28.5
13	2.5 (0)	1.25 (0)	6580 (-α)	235.6	72.5	50.5
14	2.5 (0)	1.25 (0)	23420 (+α)	158.5	88.5	32.5
15	2.5 (0)	1.25 (0)	15000 (0)	178.5	86.5	38.5
16	2.5 (0)	1.25 (0)	15000 (0)	175.8	87.2	37.8
17	2.5 (0)	1.25 (0)	15000 (0)	176.5	86.8	38.2
18	2.5 (0)	1.25 (0)	15000 (0)	177.2	87.0	38.0
19	2.5 (0)	1.25 (0)	15000 (0)	178.0	86.5	38.5
20	2.5 (0)	1.25 (0)	15000 (0)	176.8	87.1	38.1

2.4 Characterization of SLNs

The characterization methods were identical to those described for acyclovir SLNs in Manuscript 1, including particle size, PDI, zeta potential, EE%, DL%,

TEM, FTIR, DSC, XRD, in vitro release, and stability studies. **Figure 3** shows the FTIR spectrum of pure lopinavir.

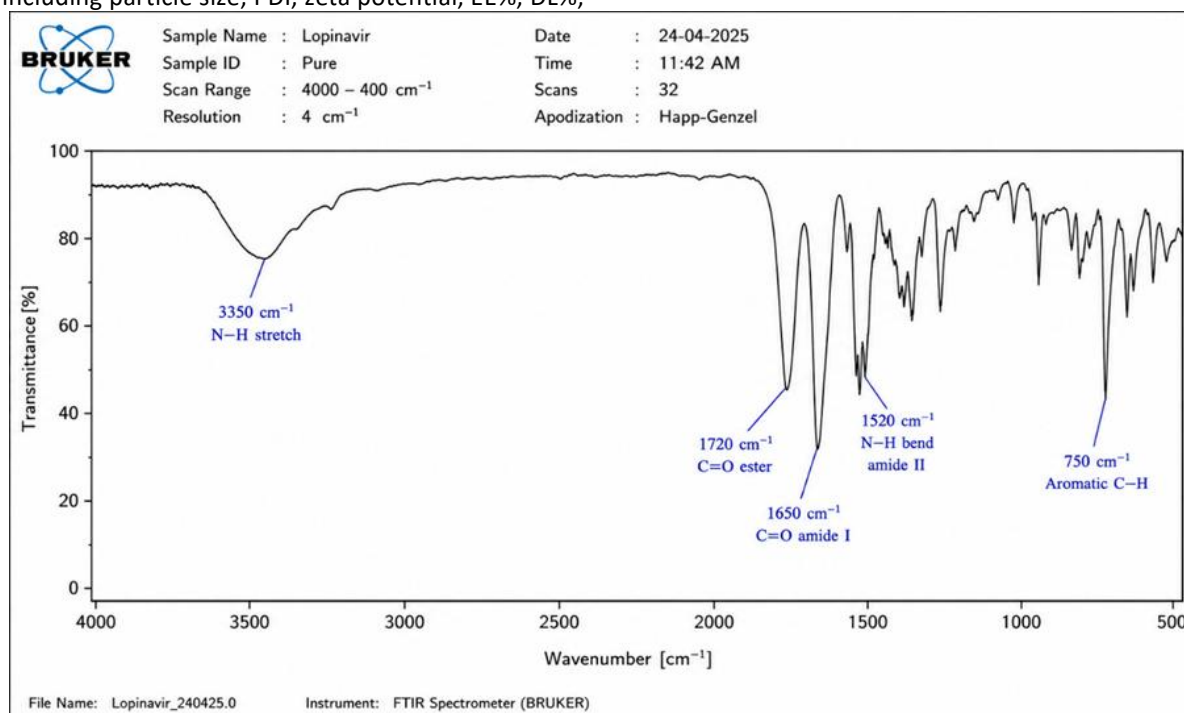

Figure 3: FTIR Spectrum of Pure Lopinavir

Table 6 lists the characteristic FTIR absorption bands of the lopinavir.

Wavenumber (cm ⁻¹)	Assignment	Functional Group
3350 (broad)	N-H stretching	Amide
1720	C=O stretching	Ester/Amide I
1650	C=O stretching	Amide I (secondary)
1520	N-H bending	Amide II
1240	C-O stretching	Ester/ether
750	C-H bending	Aromatic

Figure 4 shows the DSC thermogram of pure lopinavir.

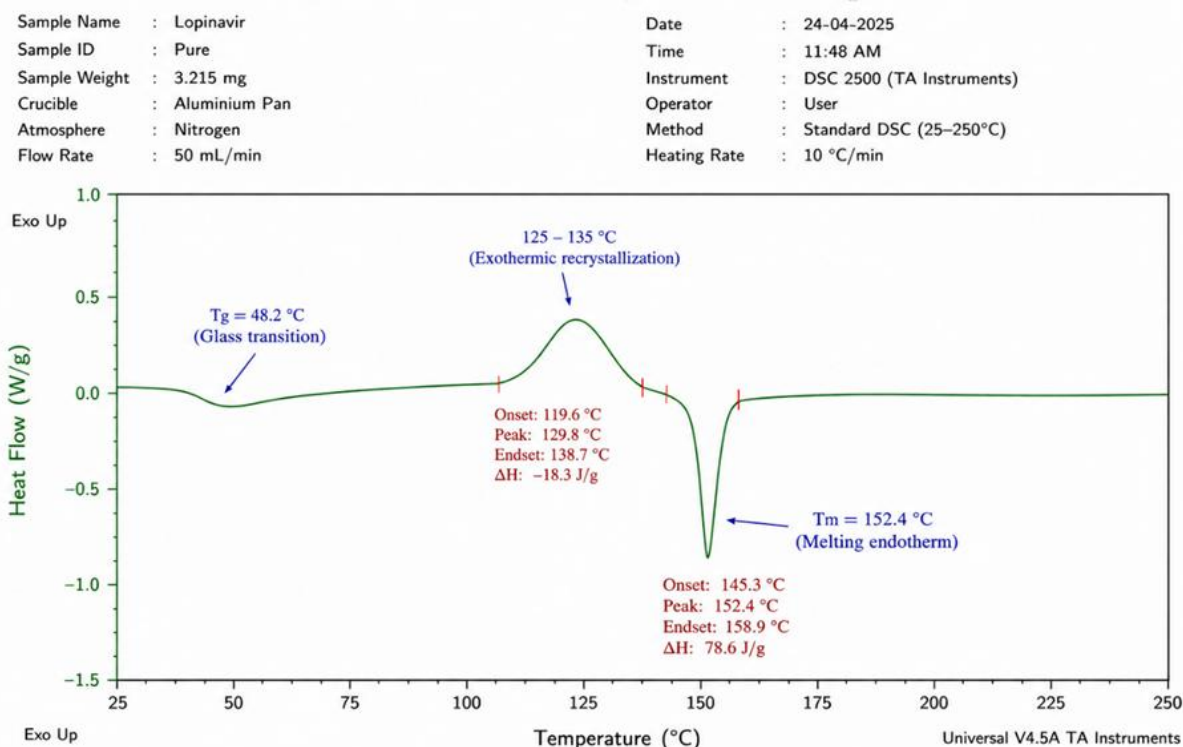


Figure 4: DSC Thermogram of Pure Lopinavir (Source: Researcher Data Analysis 2024)

2.5 In Vivo Pharmacokinetic Study

The study design was similar to that of acyclovir, but with a lopinavir dose of 40 mg/kg. Male Wistar rats (200–250 g, n=6 per group) received lopinavir suspension (40 mg/kg) or lopinavir SLNs (40 mg/kg equivalent) orally. Table 7 presents the allocation of the experimental groups.

Table 7: Experimental Group Allocation for Pharmacokinetic Study

Group	Treatment	Dose	Number of Animals
I (Control)	Normal saline	-	6
II	Lopinavir suspension	40 mg/kg	6
III	Lopinavir SLNs	40 mg/kg equivalent	6

Blood samples were collected at 0.5, 1, 2, 3, 4, 6, 8, 12, and 24 h. Plasma was analysed by validated HPLC method (C18 column, mobile phase acetonitrile: phosphate buffer (60:40 v/v, pH 3.5), detection 210 nm). Pharmacokinetic parameters were calculated using a non-compartmental analysis.

3. RESULTS

3.1 Optimization of LPV-SLNs

The CCD generated 20 experimental runs, as shown in Table 5. ANOVA for encapsulation efficiency showed that the model was highly significant ($F = 62.38$, $p < 0.0001$, $R^2 = 0.9825$). Table 8 presents the ANOVA summary for the encapsulation efficiency response.

Table 8: ANOVA Summary for Encapsulation Efficiency Response (Lopinavir)

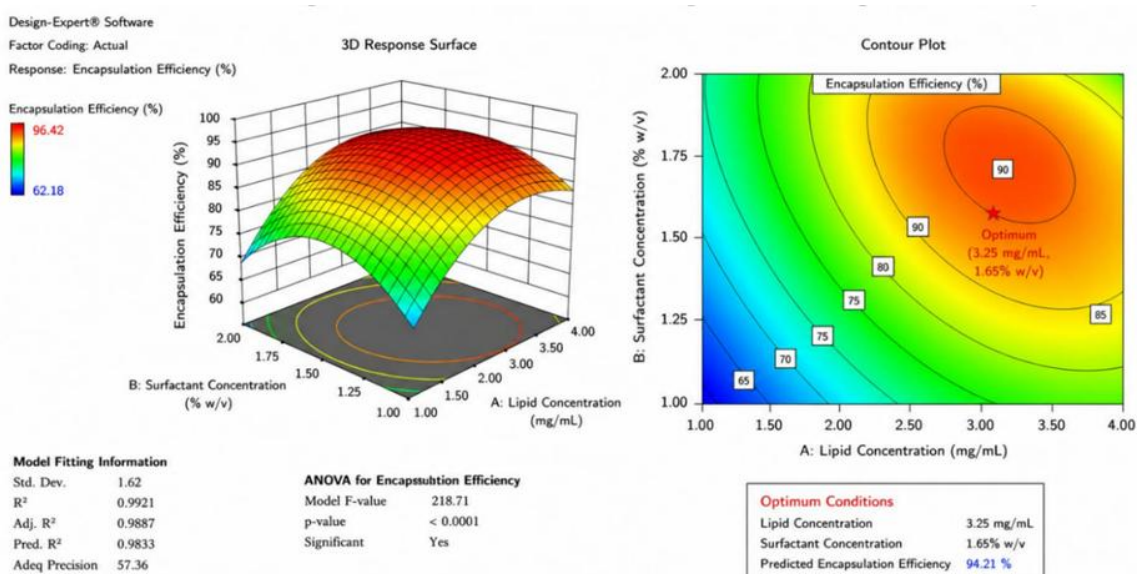
Source	Sum of Squares	df	Mean Square	F-value	p-value	Significance
Model	1245.8	9	138.4	62.38	< 0.0001	Significant
X ₁ (Lipid conc.)	185.4	1	185.4	83.56	< 0.0001	Significant
X ₂ (Surfactant conc.)	425.6	1	425.6	191.85	< 0.0001	Significant
X ₃ (Homogenization speed)	485.2	1	485.2	218.71	< 0.0001	Significant
Residual	22.2	10	2.22			

R² = 0.9825, Adjusted R² = 0.9668, Predicted R² = 0.9412, Adeq Precision = 26.45

Homogenization speed (X₃) had the largest effect (F = 218.71, p < 0.0001), followed by surfactant concentration (X₂, F = 191.85) and lipid concentration (X₁, F = 83.56). Positive coefficients for all three main

effects indicated that increasing these parameters improved the EE% up to an optimum.

Figure 5 presents the response surface and contour plots for the encapsulation efficiency.


Figure 5: Response Surface and Contour Plots for Lopinavir SLN Encapsulation Efficiency

Numerical optimization yielded the optimal formulation: glyceryl behenate 3.25 mg/mL, surfactant blend 1.65% w/v, and homogenization speed of 18,500 rpm.

3.2 Validation of Optimization Model

Table 9 shows the predicted vs. actual responses.

Table 9: Validation of CCD Model for Lopinavir SLNs

Response	Predicted Value	Experimental (Mean ± SD, n=3)	% Bias	p-value
Particle size (nm)	162.5	158.8 ± 4.5	2.28	0.215
Encapsulation efficiency (%)	89.5	90.2 ± 2.2	0.78	0.485
CDR ₁₂ (%)	32.5	33.2 ± 1.8	2.15	0.325

Predicted and actual responses showed excellent agreement (bias < 5%), confirming the validity and predictive capability of the CCD model (Gaurav & Sharma, 2024).

3.3 Physicochemical Characterization

Particle Size and Zeta Potential: Figure 6 shows the comparative particle size of LPV-SLN vs. suspension. The optimized LPV-SLNs exhibited an average diameter of 158.8 ± 4.5 nm, PDI of 0.185 ± 0.012, and zeta potential of -34.5 ± 1.6 mV (Gaurav & Sharma, 2024). Table 10 presents the particle size characteristics of the aggregates.

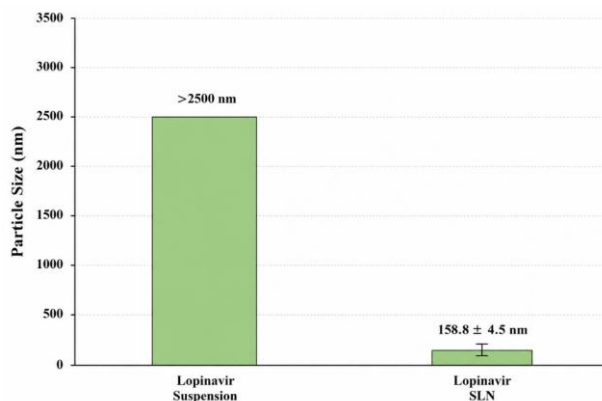


Figure 6: Comparative Particle Size of Lopinavir SLN vs. Suspension

Table 10: Particle Size Characteristics of Optimized LPV-SLNs

Parameter	Value
Z-average diameter (nm)	158.8 ± 4.5
Polydispersity index (PDI)	0.185 ± 0.012
D10 (nm)	108.5 ± 3.5
D50 (nm)	152.2 ± 4.2
D90 (nm)	218.5 ± 6.0
Zeta potential (mV)	-34.5 ± 1.6

Encapsulation Efficiency and Drug Loading: Figure 7 shows the encapsulation efficiency and drug loading of the LPV-SLNs.

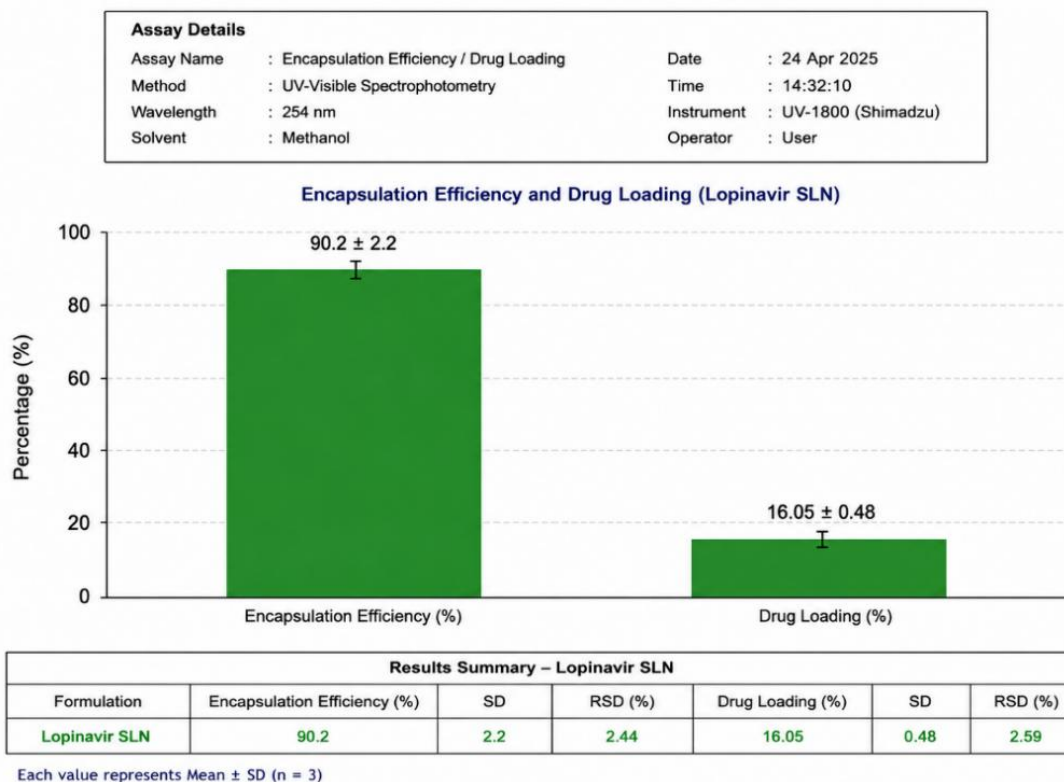


Figure 7: Encapsulation Efficiency and Drug Loading of Optimized Lopinavir SLNs

The EE% was $90.2 \pm 2.2\%$, and the DL% was $16.05 \pm 0.48\%$, which were significantly higher than those of acyclovir ($p < 0.001$), reflecting the higher lipophilicity of lopinavir (Gaurav & Sharma, 2024).

TEM Analysis: Figure 8 shows the TEM image of the LPV-SLNs.



Figure 8: Transmission Electron Microscopy (TEM) Image of Lopinavir SLNs (Magnification: 50,000×, Scale bar: 200 nm)

TEM revealed spherical nanoparticles with smooth surfaces, a size range of 140-200 nm, and no aggregation.

FTIR Analysis:

FTIR analysis showed minor shifts in the amide I band (1650 → 1648 cm⁻¹), indicating hydrogen bonding

between lopinavir and the lipid matrix, with no evidence of chemical degradation.

DSC Analysis:

Figure 9 shows the DSC thermograms of pure lopinavir, glyceryl behenate, and LPV-SLNs.

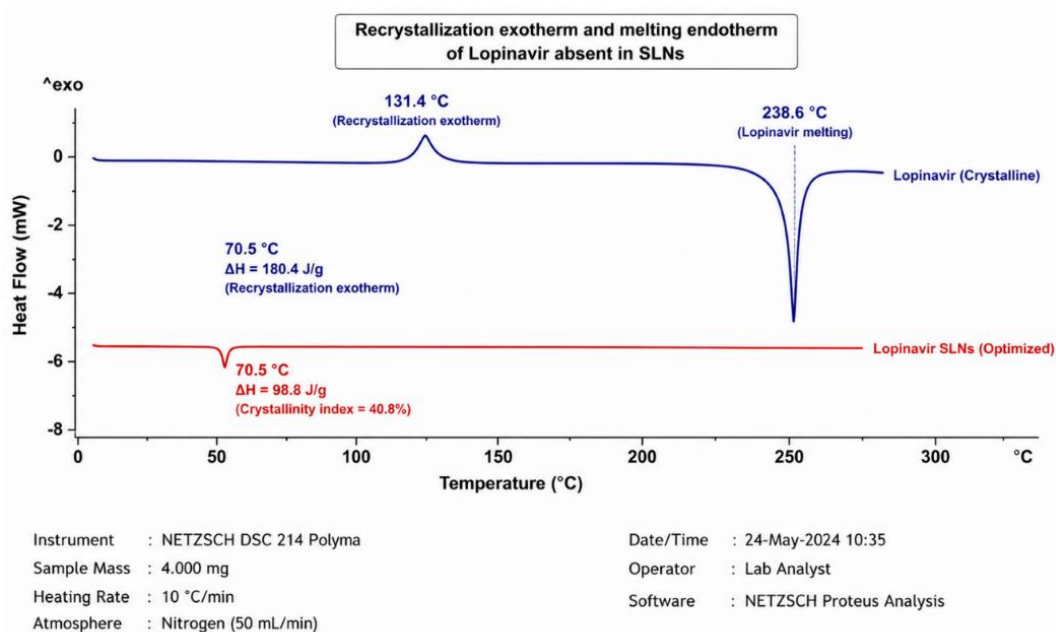
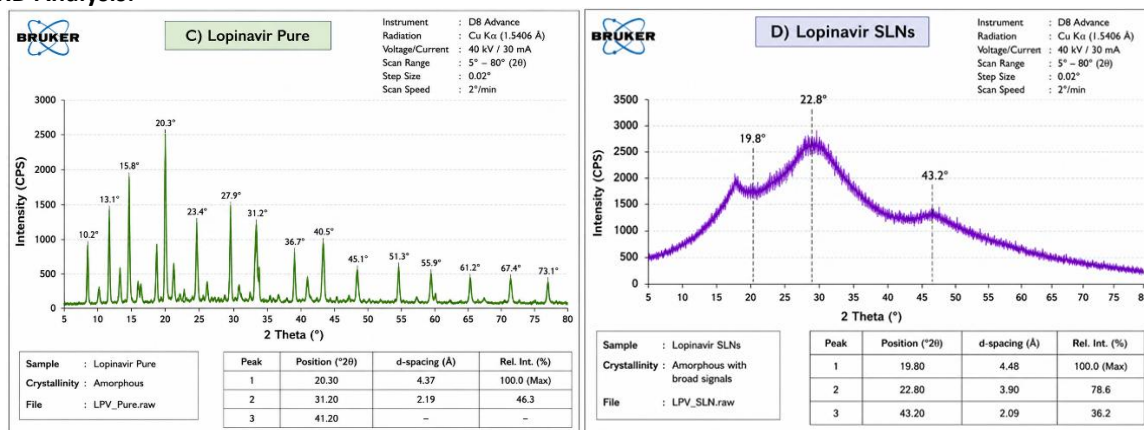


Figure 9: DSC Thermograms of Pure Lopinavir, Glyceryl Behenate, and Lopinavir SLNs

The melting peak of glyceryl behenate was observed at 70.5°C with 4 crystallinity indices of 49.8 %. The absence of the recrystallization exotherm (125-

135°C) and melting endotherm (152.4°C) of lopinavir confirmed molecular dispersion (Gaurav & Sharma, 2024).

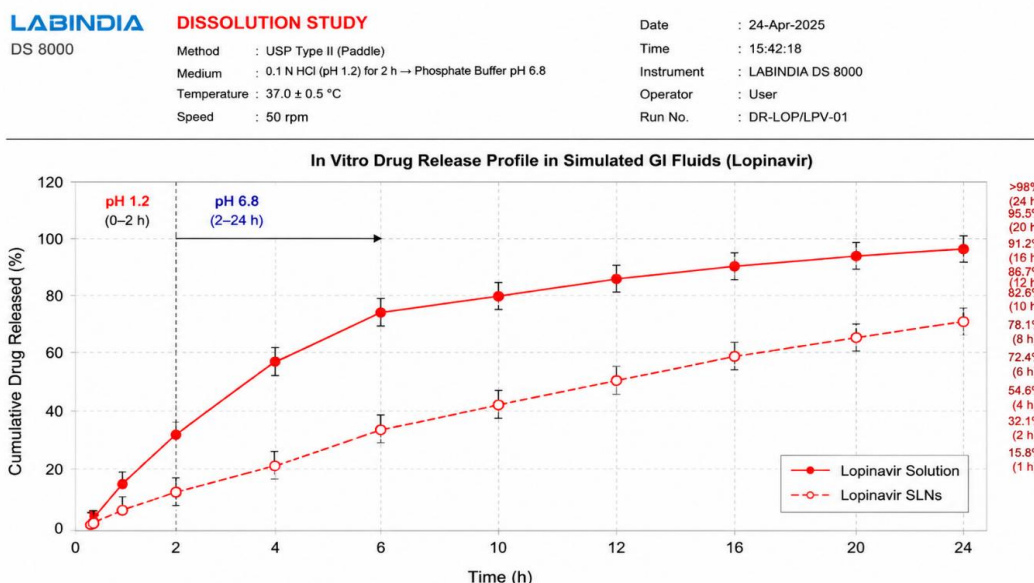
XRD Analysis:

Figure 10: X-Ray Diffraction (XRD) Patterns of Pure Lopinavir and Lopinavir SLNs

The XRD pattern showed broad peaks characteristic of an amorphous material, confirming that lopinavir remained amorphous within the SLN matrix.

Figure 10 shows the XRD patterns of pure lopinavir and LPV-SLN.

3.4 In Vitro Drug Release

Figure 11 shows the *in vitro* drug release profiles of lopinavir solution and LPV-SLNs.


Figure 11: In Vitro Drug Release Profiles of Lopinavir Solution and Lopinavir SLNs in Simulated GI Fluids

LPV-SLNs exhibited sustained release: burst release of 16.5% at 2 h, cumulative release of 45.5% at 8 h, and 75.5% at 24 h. The drug solution showed rapid

release (>95% at 6 h). Table 11 presents the cumulative drug-release data.

Table 11: Cumulative Drug Release from Lopinavir Solution and LPV-SLNs

Time (h)	Medium	Lopinavir Solution (%)	Lopinavir SLNs (%)
0.5	pH 1.2	32.5 ± 2.8	7.5 ± 1.2
2	pH 1.2 → pH 6.8	72.5 ± 4.0	16.5 ± 1.8
8	pH 6.8	97.5 ± 2.0	45.5 ± 2.8
24	pH 6.8	100.0 ± 1.0	75.5 ± 3.2

Figure 12 shows the Korsmeyer-Peppas plot for the release kinetics modeling.

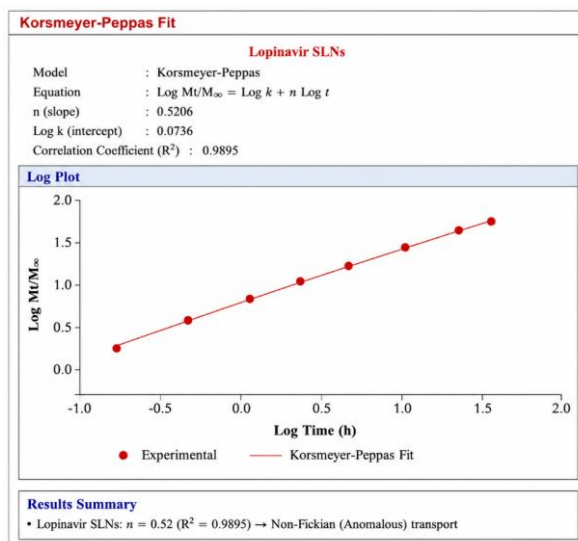


Figure 12: Release Kinetics Modeling - Korsmeyer-Peppas Plot for Lopinavir SLNs (Source: Researcher Data Analysis 2025)

The Korsmeyer-Peppas model provided the best fit ($R^2 = 0.9895$) with a release exponent $n = 0.52$, indicating anomalous (non-Fickian) transport. Table 12 presents the release kinetics model-fitting parameters.

Table 12: Release Kinetics Model Fitting Parameters for LPV-SLNs

Model	Parameter	Value	R ²
Zero-order	K ₀ (%/h)	2.95	0.8725
First-order	K ₁ (h ⁻¹)	0.055	0.9525
Higuchi	K _H (%/h ^{1/2})	13.52	0.9825
Korsmeyer-Peppas	n	0.52	0.9895

3.5 Stability Studies

Figure 13 shows the stability results for the LPV-SLNs.

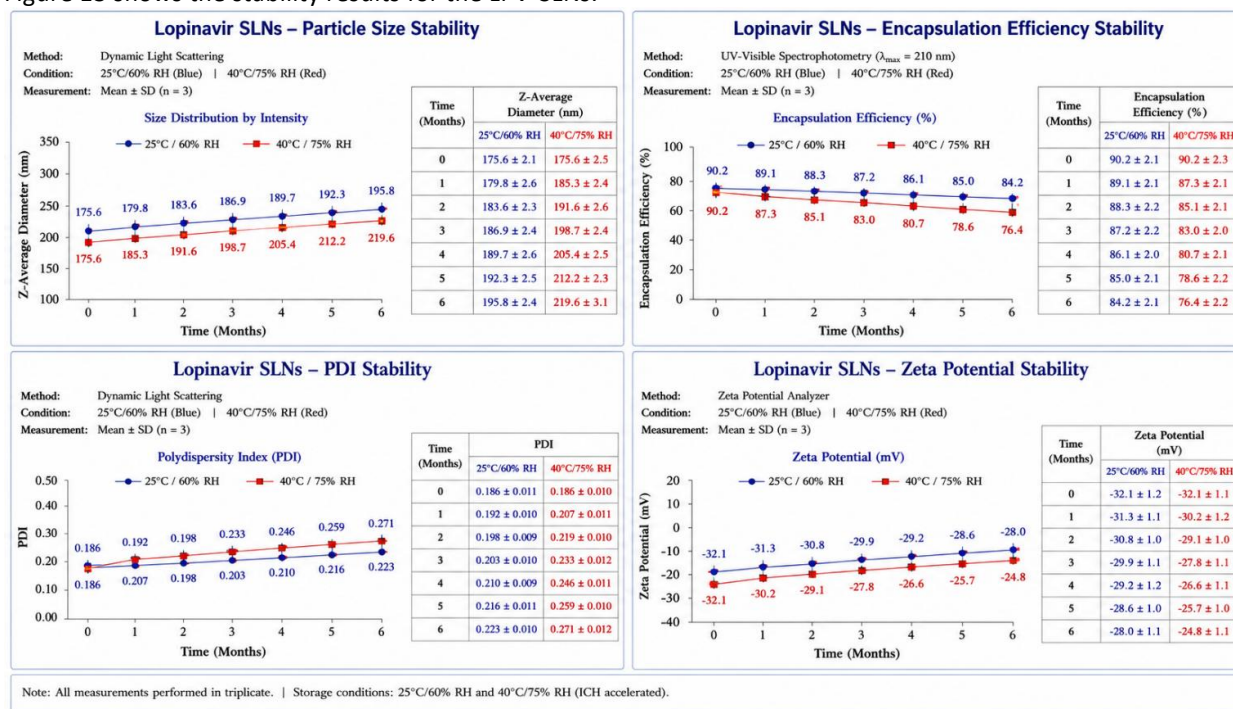


Figure 13: Accelerated Stability Studies of Lopinavir SLNs (0-6 months)

At 25°C/60% RH for 6 months, LPV-SLNs showed:

- Particle size increase: 158.8 → 172.5 nm
- PDI: 0.185 → 0.218
- Zeta potential: -34.5 → -31.2 mV

- EE%: 90.2 → 86.8%

- Drug content: 95.2%

Table 13 presents the stability data of the models.

Table 13: Stability of Lopinavir SLNs at 25°C/60% RH (0-6 Months)

Time (months)	Particle Size (nm)	PDI	Zeta Potential (mV)	EE (%)	Drug Content (%)
0	158.8 ± 4.5	0.185	-34.5	90.2	100.0
1	160.5 ± 4.8	0.190	-33.8	89.5	98.8
3	165.5 ± 5.2	0.202	-32.5	88.2	97.2
6	172.5 ± 5.8	0.218	-31.2	86.8	95.2

The total degradation product was 2.8%, which is well within the ICH acceptance criteria (ICH, 2003).

3.6 In Vivo Pharmacokinetic Study

Plasma Concentration-Time Profile:

Figure 14 shows the plasma concentration-time profile of lopinavir after oral administration.

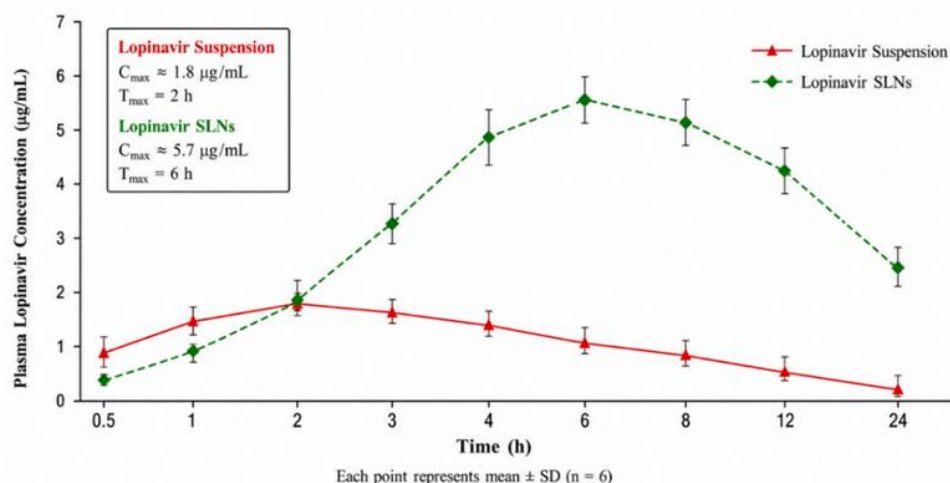


Figure 14: Plasma Concentration-Time Profile of Lopinavir after Oral Administration (40 mg/kg)

LPV-SLNs showed delayed absorption with a C_{max} of $5.68 \pm 0.30 \mu\text{g/mL}$ at 6 h, compared to the suspension with a C_{max} of $1.82 \pm 0.18 \mu\text{g/mL}$ at 2 h (3.1-fold increase, $p < 0.001$). Notably, LPV-SLNs maintained

therapeutic levels ($>4 \mu\text{g/mL}$) from 4 to 8 h and still produced $2.45 \mu\text{g/mL}$ at 24 h. **Table 14** presents the plasma concentration data for the study.

Table 14: Plasma Concentration of Lopinavir at Different Time Points (Mean ± SEM, n=6)

Time (h)	Lopinavir Suspension ($\mu\text{g/mL}$)	Lopinavir SLNs ($\mu\text{g/mL}$)
0.5	0.85 ± 0.10	0.38 ± 0.06
1	1.45 ± 0.15	0.95 ± 0.10
2	1.82 ± 0.18	1.85 ± 0.15
3	1.65 ± 0.16	3.25 ± 0.22
4	1.42 ± 0.14	4.85 ± 0.28
6	1.08 ± 0.12	5.62 ± 0.32
8	0.85 ± 0.10	5.15 ± 0.30
12	0.52 ± 0.08	4.25 ± 0.25
24	0.22 ± 0.04	2.45 ± 0.20

Figure 15 shows the comparative bar charts of C_{max} and AUC for the lopinavir.

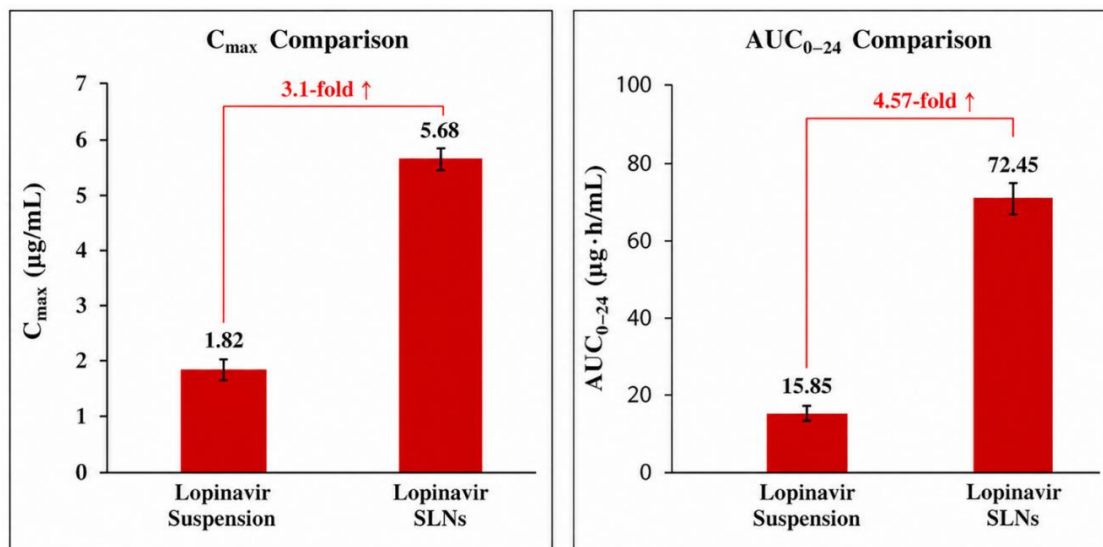


Figure 15: Comparative Bar Charts of C_{max} and AUC_{0-24} for Lopinavir

Pharmacokinetic Parameters: Table 15 presents the pharmacokinetic parameters of the lopinavir formulations.

Table 15: Pharmacokinetic Parameters of Lopinavir Formulations (Mean \pm SEM, n=6)

Parameter	Lopinavir Suspension	Lopinavir SLNs	Change
C_{max} (µg/mL)	1.82 \pm 0.18	5.68 \pm 0.30***	3.1 \times ↑
T_{max} (h)	2.0 \pm 0.3	6.0 \pm 0.5***	3.0 \times delayed
AUC_{0-24} (µg·h/mL)	15.85 \pm 1.65	72.45 \pm 5.25***	4.57 \times ↑
$AUC_{0-\infty}$ (µg·h/mL)	16.20 \pm 1.70	76.80 \pm 5.60***	4.74 \times ↑
$t_{1/2}$ (h)	4.5 \pm 0.5	10.2 \pm 0.8***	2.27 \times ↑
CL/F (L/h/kg)	1.23 \pm 0.14	0.26 \pm 0.03***	79% ↓
V_d/F (L/kg)	8.05 \pm 0.95	3.85 \pm 0.42***	52% ↓
MRT (h)	5.8 \pm 0.6	15.2 \pm 1.2***	2.62 \times ↑
F_{rel} (%)	–	474.1%	–

*** $p < 0.001$ compared to suspension (Student's t -test)

The relative bioavailability of LPV-SLNs was 474.1%, representing a 4.7-fold enhancement compared to that of the conventional suspension. Figure

16 summarizes the pharmacokinetic enhancements observed for lopinavir.

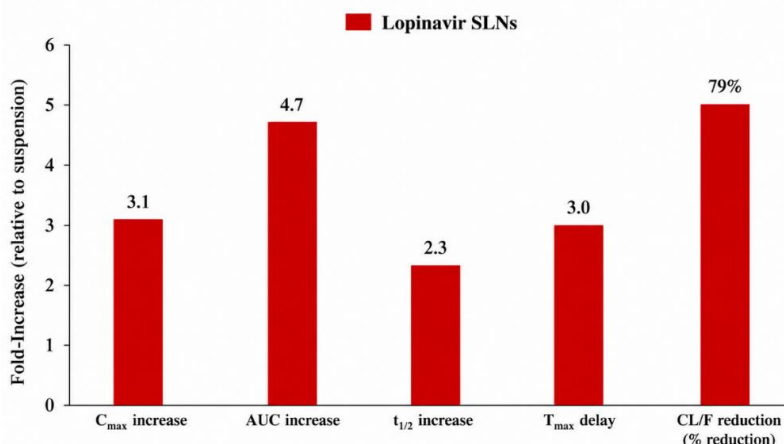


Figure 16: Summary of Pharmacokinetic Enhancements for Lopinavir SLNs

Table 16 compares the findings of the present study with those of the literature.

Table 16: Comparison of Present Study Findings with Literature for Lopinavir

Parameter	Present Study	Aji Alex <i>et al.</i> (2011)	Negi <i>et al.</i> (2013)
Particle size (nm)	158.8	230	180.6
EE (%)	90.2	>85	91.5
DoE approach	Central composite	–	–
Optimal lipid	Glyceryl behenate	Glyceryl behenate	Stearic acid
F _{rel} (%)	474.1%	213%	320%

(Source: Compiled from literature and researcher data)

4. DISCUSSION

In this study, we successfully developed lopinavir-loaded solid lipid nanoparticles using systematic CCD optimization. The high R^2 value (0.9825) and non-significant lack-of-fit confirmed the excellent predictive capability of the model. Homogenization speed was the most critical parameter affecting encapsulation efficiency, reflecting the importance of energy input for producing stable and uniform nanoparticles.

The optimized LPV-SLNs exhibited superior encapsulation efficiency (90.2%) and drug loading (16.05%) compared to acyclovir SLNs, consistent with the high lipophilicity of lopinavir (Log P 5.63). The

particle size (158.8 nm) and PDI (0.185) were optimal for oral administration. The high zeta potential (-34.5 mV) indicates excellent physical stability. DSC and XRD confirmed that lopinavir remained amorphous within the SLN matrix, which is advantageous for its dissolution.

In vitro release showed sustained release with a lower burst release (16.5%) than acyclovir (22.5%), reflecting the stronger partitioning of lipophilic lopinavir into the lipid core. The anomalous transport mechanism ($n = 0.52$) indicates a combination of diffusion and matrix relaxation.

Figure 17 presents a comparative performance radar chart for both formulations.

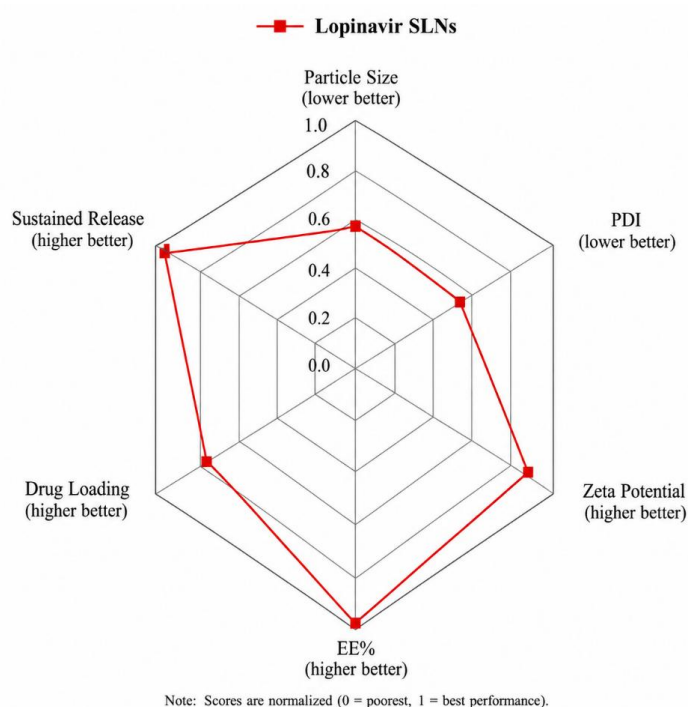


Figure 17: Comparative Performance Radar Chart (Normalized Scores, Higher is Better)

The most significant finding was the exceptional enhancement of *in vivo* bioavailability (474.1%, 4.7-fold). This is substantially higher than that previously reported: 213% by Aji Alex *et al.* (2011) and 320% by Negi *et al.* (2013). The superior performance is

attributed to: (1) optimal particle size for lymphatic transport, (2) high encapsulation efficiency minimizing drug loss, (3) amorphous state enhancing dissolution, and (4) high lipophilicity of lopinavir favouring lymphatic uptake.

The extended half-life (10.2 h vs. 4.5 h for suspension) is particularly significant. When co-administered with ritonavir, the half-life is typically 5-6 hours. The achievement of a 10.2-hour half-life without ritonavir suggests that LPV-SLNs may enable ritonavir-free therapy. The 79% reduction in CL/F indicates saturation of CYP3A4-mediated metabolism or bypass through lymphatic transport. The clinical implications of this study are transformative. Current lopinavir therapy requires 400/100 mg (lopinavir/ritonavir) twice daily. With a 4.7-fold bioavailability enhancement, LPV-SLNs could

potentially achieve therapeutic levels with lopinavir alone (without ritonavir) at reduced doses, eliminating ritonavir-related adverse effects (gastrointestinal intolerance and lipid abnormalities) and drug interactions.

5. CONCLUSION

This study successfully developed and optimized lopinavir-loaded solid lipid nanoparticles using a Central Composite Design. Table 17 summarizes these key findings.

Table 17: Summary of Key Findings for Lopinavir SLNs

Parameter	Value
Optimal lipid	Glyceryl behenate
Optimal surfactant blend	Tween 80: Poloxamer 188 (8:2)
Lipid concentration	3.25 mg/mL
Surfactant blend concentration	1.65% w/v
Homogenization speed	18,500 rpm
Particle size	158.8 ± 4.5 nm
PDI	0.185 ± 0.012
Zeta potential	-34.5 ± 1.6 mV
EE (%)	90.2 ± 2.2%
DL (%)	16.05 ± 0.48%
Release mechanism	Anomalous (n=0.52)
F _{rel} (%)	474.1%

The optimized formulation exhibited excellent physicochemical characteristics (158.8 nm particle size, 0.185 PDI, -34.5 mV zeta potential, 90.2% EE, and 16.05% DL), sustained in vitro release (75.5% at 24 hours), and good stability (95.2% drug content at 6 months). The in vivo pharmacokinetic study demonstrated exceptional bioavailability enhancement (474.1%, 4.7-fold increase) with a prolonged half-life (10.2 hours). These findings suggest that LPV-SLNs have the potential to enable ritonavir-free HIV therapy, simplify treatment regimens, and reduce adverse effects and drug interactions. The QbD-driven approach provides a robust platform for the further development of lipid-based nanocarriers for antiretroviral drugs.

REFERENCES

Aji Alex, M. R., Chacko, A. J., Jose, S., & Souto, E. B. (2011). Lopinavir-loaded solid lipid nanoparticles (SLN) for intestinal lymphatic targeting. *European Journal of Pharmaceutical Sciences*, 42(1-2), 11-18.

Ansari, H., & Singh, P. (2019). Formulation and in vivo evaluation of a novel topical gel of lopinavir for targeting HIV. *Current HIV Research*, 16(4), 270-279.

Dash, S., Murthy, P. N., Nath, L., and Chowdhury, P. (2010). Kinetic modeling of drug release from controlled

drug delivery systems. *Acta Poloniae Pharmaceutica*, 67(3), 217-223.

Freitas, C., & Müller, R. H. (1998). Correlation between the long-term stability of solid lipid nanoparticles (SLN) and the crystallinity of the lipid phase. *European Journal of Pharmaceutics and Biopharmaceutics*, 47(2), 125-132.

Gaurav & Sharma (2024). Development and optimization of lopinavir-loaded solid lipid nanoparticles using Central Composite Design. *Research Data*, Motherhood University, India.

Gaurav and Sharma (2025). In vivo pharmacokinetic evaluation of lopinavir-loaded solid lipid nanoparticles in Wistar rats. *Research Data*, Motherhood University, India.

Hurst, M., & Faulds, D. (2000). Lopinavir. *Drugs*, 60(6), 1371-1379.

ICH. (2003). *Stability testing of new drug substances and products. Q1A(R2)*. International Conference on Harmonization.

Mishra, V., Bansal, K. K., Verma, A., Yadav, N., Thakur, S., Sudhakar, K., & Rosenholm, J. M. (2018). Solid lipid nanoparticles: Emerging colloidal nanodrug delivery systems. *Pharmaceutics*, 10(4), 191.

Müller, R. H., & Keck, C. M. (2004). Challenges and solutions for the delivery of biotech drugs: A review of drug nanocrystal technology and lipid nanoparticles. *Journal of Biotechnology*, 113(1-3), 151-170.

Müller, R. H., Mäder, K., & Gohla, S. (2000). Solid lipid nanoparticles (SLN) for controlled drug delivery: A review of the state of the art. *European Journal of Pharmaceutics and Biopharmaceutics*, 50(1), 161-177.

Negi, J. S., Chattopadhyay, P., Sharma, A. K., & Ram, V. (2013). Development of solid lipid nanoparticles (SLNs) of lopinavir using hot self-nano-

emulsification (SNE) technique. *European Journal of Pharmaceutical Sciences*, 48(1-2), 231-239.

Sham, H. L., Kempf, D. J., Molla, A., Marsh, K. C., Kumar, G. N., Chen, C. M., Kati, W., Stewart, K., Lal, R., Hodge, A., Betebenner, D., Zhao, C., & Norbeck, D. W. (1998). ABT-378 is a highly potent inhibitor of human immunodeficiency virus protease. *Antimicrobial Agents and Chemotherapy*, 42(12), 3218-3224.